International Journal of Engineering Innovation & Research
Volume 7, Issue 2, ISSN: 2277 – 5668

Experimental Measurement of Flow Field using Three Dimensional Visualization Method

Rajendra Shrestha
Department of Mechanical Engineering, Pulchowk Campus, Institute of Engineering, Tribhuvan University, Lalitpur, Nepal
Corresponding author email id: rsfluid@hotmail.com

Date of publication (dd/mm/yyyy): 17/04/2018

Abstract **– Cavitation and coalescence of bubbles are transient in characters and inevitable in Hydropower stations operated with Francis turbines. However, there are challenges in measurement of these phenomena. In this research measurement of flow field is carried by using three dimensional visualization method. This technique has been developed to study the flow regions, which are generally so small and transient that the normal flow would greatly disturbed and perhaps disappears if probes are introduced to measure the flow field. In this research flow field (10 mm/s velocity) around continuously rising bubbles in stagnant water pool were experimentally measured using Orgasol-2002 ES6 NAT3 tracer, camera of different shutter speeds and Argon laser. Further dimension and positions of 0.2 to 1.5 mm bubbles were measured using CCD camera with stroboscope as back lighting and mirrors as splitting images.**

Keywords **– Bubble Trains, Flow Pattern, Laser Sheet, Particle Image Velocimetry, Tracer.**

I. Introduction

Measurement of fluid flow include the determination of pressure, velocity, discharge, shock wave, density gradient, turbulence, viscosity, flow field, vortex etc. Flow visualization method measures the motion of small, marked region of fluid by observing the locations of the images of the marks (tracers) at different times. Regardless of marker type, locations at various instants are recorded optically by laser light that freezes the marked images on an optical recording medium such as a photographic film, a video camera detector etc. A technique that uses particles and their images falls into the category commonly known as particle image velocimetry (PIV).

Different experimental things such as properties of the marking tracer, illumination, resolution, image-density, should be analyzed for its application in the specific fields. Analysis of the recorded images is one of the most important steps in the entire process, as it couples with the image-acquisition process to determine the accuracy, reliability, and spatial resolution of the measurements.

In this paper the process of experiment and recording of images were explained in detail. The flow field (which were around 10 mm/sec) developed by the rising nitrogen bubbles in stagnant water were observed successfully, by seeding the tracer in water.

II. Methodology

Many experimental techniques have been developed and employed for the measurement of flow fields. In general, the measurement techniques can be classified into two categories depending on the nature of sensors contacting the flow fields, namely internal sensors and external sensors [7]. Internal sensors include probes, such as optical probes and static probes. External sensors include photographic, X-ray and γ-ray methods. In the present experiment, visualization method followed by image processing method was performed, using CCD video camera and still camera to observe flow field around the bubble trains.

2.1 Measurements of Dimensions and Positions of Bubble Trains

Dimensions of bubbles were carried out by image processing procedure of the graphic data taken by CCD video camera (30 frames per second) with stroboscope as the back lighting as shown in Fig. 1. The frequency of the stroboscope was set at 120 Hz to obtain the double exposed images per frame. Different rising pattern and resulting flow fields were determined; bubbles rose straight upward, branching in inclined path or zigzag paths.

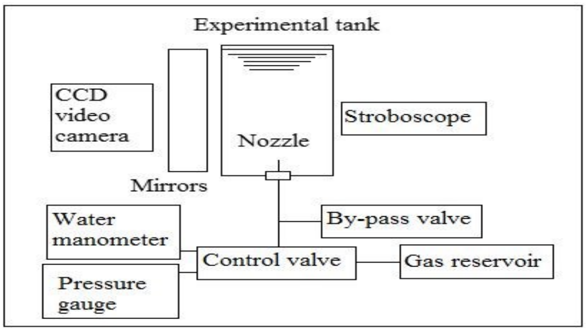

Fig. 1 Schematic diagram of experimental setup

The ranges of bubble diameters and Reynolds numbers obtained were between 0.2 mm to 1.5 mm, and between 10 to 310, respectively. Measured ranges of rising velocities were 47 mm/s to 206 mm/s, generation frequencies were 7.4 Hz to 37.89 Hz and mutual bubble distances were 1.2 mm to 25 mm.

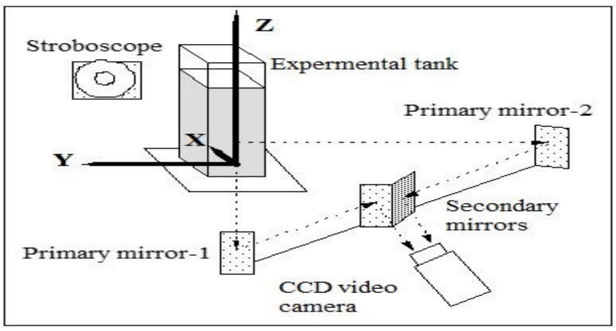

Fig. 2 Schematic diagram of stereo image observation setup

International Journal of Engineering Innovation & Research
Volume 7, Issue 2, ISSN: 2277 – 5668

The bubble rising patterns were observed three-dimensionally using four mirrors, so called "split mirror method" used by Murai et al. [3] as shown in Fig. 2. The frequency of the stroboscope, which was located at the back of the experimental tank as the back lighting, was set as 60 Hz. The images of the two side views of the rising bubbles were reflected first by two primary mirrors attached on the sides of the experimental tank, then reflected by two secondary mirrors, to the CCD video camera in front of the experimental tank. The mirrors were so arranged that the images of two perpendicular sides of the test section could be obtained in two halves of a single frame and each image was exposed once per frame. These images were converted into Microsoft bitmap files (320 × 240 pixels), and processed for the positions of the bubble centers. The three dimensional positions of bubbles were determined using images obtained by using split mirrors, is shown in Fig. 3 along X-Z, Y-Z and X-Y planes.

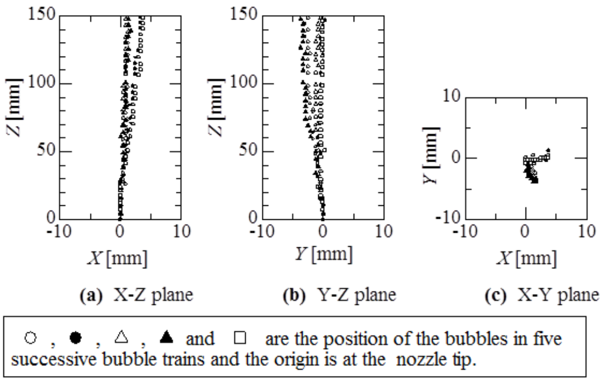

Fig. 3 Three-side views of trajectories of 0.85 mm bubble trains

III. Flow Field Generated by Rising Bubbles

The flow field development by the bubble trains was observed, by seeding the tracer in the water. Argon laser sheet of 1.00 mm thickness was used for slicing the three-dimensional flow field. As the data recording devices, both the CCD video camera with the recording frequency of 30 Hz and the still camera with different shutter speeds were used to take the images. Detail observations were done by careful analysis of both CCD video camera recording and steel camera images. The optimum view heights were set to be between 30 mm to 80 mm, to record the flow fields both in the large scale and in the small scale.

Several kinds of tracers having the characteristics of relative density close to unity, inertness, smaller diameter and better visibility were tested. The four kinds of the tracers were selected for the observation of the flow fields. Polystyrene particles (Diaion-HP20) with 0.400 ± 0.100 mm diameter, the relative density of which was equal to 1.02, to obtain clear trace of the flow field. It was found that some tracer particles were disturbing the rising bubbles. Next, the highly reflective particle (Metallic Coated Particles – 10087) with 0.012 ± 0.001 mm diameter was tested, the relative density of which was equal to 2.60. These particles have good refractive index however, the excessive use of them tended to promote the frequent change of the bubble rising directions. Then, nylon particle (Vestosint - 2070) with 0.005 ± 0.002 mm diameter was used, the relative density of which was equal to 1.03. It was found that their diameters were too small to reflect the light with given power and they were useful only when the close up view with the view height less than 8.00 mm. The best tracer selected for the present experiments was other nylon particle (Orgasol-2002 ES6 NAT3) with the diameter of 0.060 ± 0.003 mm, the relative density of which was equal to 1.03. These particles possessed the characteristics of the relatively clear image and less disturbing the flow field. The flow field development by different sizes of bubble trains were observed.

3.1 Flow Field Generated by 0.5 mm Diameter Bubbles

The experimental conditions were chosen to generate the bubble trains with bubble diameter as 0.5 mm and mutual distance of the bubbles as 10 mm, by using 0.02 mm nozzle and setting nozzle upstream pressure at 50 kPa. The nozzle tip was located at 80 mm height from the bottom of the tank, for the ease of the visualization. Bubbles rose along almost the same trajectories, which were close to the straight lines.

3.1.1 Flow Field in X-Z Plane

In this experiment, the laser sheet of 1.0 mm thickness was first placed on the X-Z plane including the nozzle tip. The laser sheet was introduced from the left side of the experimental tank. The photo images of the flow field generated by 0.5 mm diameters bubble trains with the shutter speed 8.0 s are shown in Figs. 4. These image was taken with the view area of 60×90 mm^2. The image was taken after the motions of bubble trains became uniform. In Fig. 4, the trajectories of bubbles are shown as the thin continuous white line, from the bottom to the top of the pictures. This continuous white line is the reflected light on the surface of the bubbles. The vertical velocities of the bubbles are positive and upward, while the lateral velocities are nearly zero.

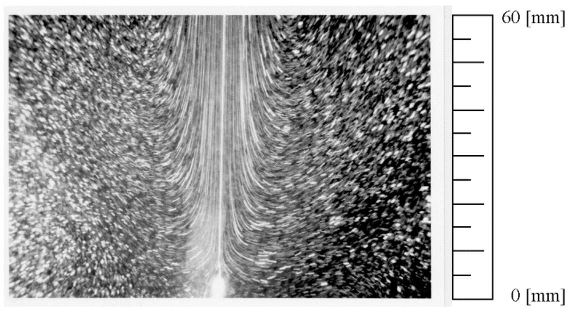

Fig. 4 Flow field generated by 0.5 mm diameter bubble trains in X-Z

In the vicinity of the both sides of the bubble trajectories, small amounts of the displacements of the tracers were observed, which are shown as the line segments aligned in the vertical direction from the bottom to the top, in Fig. 4. It should be noticed that the line segments are parallel to each other and that they are constrained to exist in a region close to the bubble trains. Both the area and the shape of this region were observed to be time-independent, as long as the bubbles rose along the almost identical path. The flow pattern was almost invariable during the experiment. This region is considered as the affective region. In this region, the velocities are vertical and toward the direction of the bubbles. The significant amount of flow was observed toward the affective region and the tracer particles were injected into the affective region. The magnitudes of the water velocities in this region are about one thirteenth to those of bubbles i.e. around 5.5 mm/s.

3.1.2 Flow Field in X-Y Plane

The X-Y plane photo images of the same flow field discussed in the previous section is shown in Figs. 5. These images were taken with the view area of 75 × 112 mm^2, and slicing X-Y plane by the laser sheet which was placed 30 mm above the nozzle tip. As verified by the CCD video camera images, the positions of the bubble motions are indicated by the centers of the circle drawn in Figs. 5.

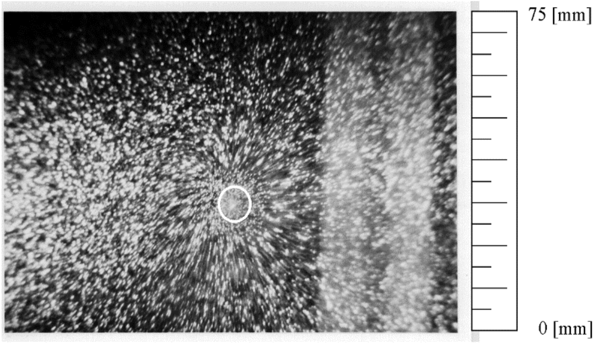

Fig. 5 Flow field generated by 0.5 mm diameter bubble trains in X-Y plane

The flow field is almost stationary in Fig. 5. By using the CCD video camera, the directions of the velocities in this region were observed to be the same as the direction of the bubbles in the trajectory. The affective region discussed in the previous section exists in this region. The surrounding flow field was observed to be attracted towards this affective region.

3.2 Flow Field Generated by 1.5 mm Diameter Bubbles

The experimental conditions were chosen as to generate bubble trains with bubble diameter as 1.5 mm and mutual distance of the bubbles as 23 mm, by using 0.10 mm nozzle and setting nozzle upstream pressure at 10 kPa. The nozzle tip was located at 70 mm height from the bottom of the tank, for the ease of the visualization. In this bubble trains, the instabilities and the three-dimensional complex motions were observed than in 0.5 mm diameter bubbles.

3.2.1 Flow Field in X-Z Plane

The laser sheet was first placed on the X-Z plane including the nozzle tip. The photo images of the flow field generated by the 1.5 mm diameter bubble trains with the shutter speeds of 4.0 s are shown in Figs. 6. The image was taken with the view area of 50 × 75 mm^2. The motions of bubbles of this bubble trains were so unstable that they were not necessarily constrained in the X-Z plane, nor in any planes. Therefore, the picture in Fig. 6 was taken when the trajectories of bubbles were observed to exist in the vicinity of the X-Z plane including the nozzle tip. The existence of bubbles in the vicinity of this plane can be verified by the fact that the reflected light on the bubble surfaces of the laser sheet of 1.0 mm thickness is clearly captured in the pictures.

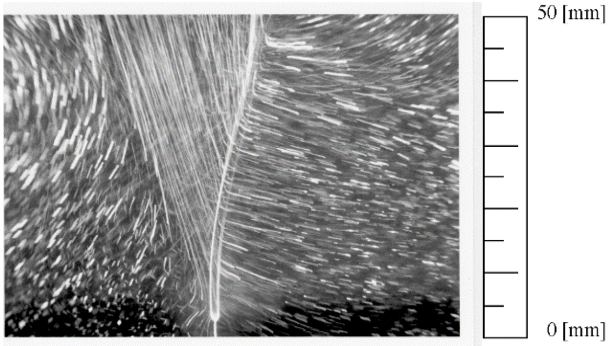

Fig. 6 Flow field generated 1.5 mm diameter bubble trains in X-Z plane

In Fig. 6, the trajectories of bubbles are shown as the thick continuous white line, from the bottom to the top of the pictures. This thick continuous white line is the reflected light on the surface of bubbles. The laser sheet was introduced from the left side of the pictures. It is possible to estimate roughly the directions of the bubble motions in the X-Z plane from Fig. 6. The vertical velocities are, of course, positive and upward, while the lateral velocities are also positive and toward the right direction.

In the vicinity of the left side of the bubble trajectories, the significant amounts of the displacements of the tracers, which are shown as the line segments aligned in the direction from the right bottom to the top left, can be observed in Fig. 6. It should be noticed that the line segments are parallel to each other and that they are constrained to exist in a certain region. Both the area and the shape of this region were observed to be time-independent, as long as the bubbles rose along the almost identical path. The flow pattern was almost invariable during the experiments. This region is referred to as the triangle region. In the triangle region, the vertical velocities of water are positive and upward, while the lateral velocities are negative and toward the left direction, which is the opposite to those of the bubbles. The magnitudes of the water velocities in the triangle region are about one fifteenth times to those of bubbles i.e. around 20 mm/s. It should be noticed that the structures of the flow field are totally different between the region right to the bubble trajectories, which is referred as the right region, and the region left to the triangle region, which is referred as the left region.

In the right region, the lateral velocities are much greater than the vertical velocities, and the dominant flow is observed toward the triangle region. The flow field in the right region injects the tracer particles into the triangle region through the boundary characterized by the bubble trajectories. It is observed that the main flow in the triangle region is supplied from the right region, and that the sudden acceleration of water is observed in the vicinity of the bubble trajectories.

In the left region, the impaling flow into the triangle region cannot be observed, but the momentum entrainment effects are significant. In this region, much less accelerations of the flow than in the right region are observed. The flow fields gradually change their directions in the vicinity of the boundary between two regions, which is not so sharp as the other one.

The structures of the flow field around the rising bubble trains are so complicated and, of course, three-dimensional. In order to obtain more information of these structures, the cross sectional pictures in X-Y plane were studied.

3.2.2 Flow Field in X-Y Plane

The X-Y plane photo image of the same flow field discussed in the previous section is shown in Fig. 7. This image was taken with the view area of 64 × 97 mm^2, and slicing X-Y plane by the laser sheet, which was placed 30 mm above the nozzle tip. This image was taken with the shutter speed of the still camera of 8.0 s. As verified by the CCD video camera images, the directions of the bubble motions are as indicated by the arrows in Fig. 7. The bubble positions in the picture is shown as the starting point of the arrow. The bubble motions were not confined in the X-Z plane when this picture was taken, hence the arrow is not parallel to the X-direction.

It can be noticed that there exists a narrow band of the tracer particles with much higher tracer number density. The width of this band, perpendicular to the direction of the arrow, is about the order of the diameter of the bubbles in the train. By using the CCD video camera, the directions of the velocities in this band were observed to be opposite to the direction of the arrow. The most striking nature of the flow field is that the triangle region discussed in the previous section exists only in this narrow band. In other words, the triangle region is observed to confined in the very restricted space. This narrow band is connected to the strong vortex region.

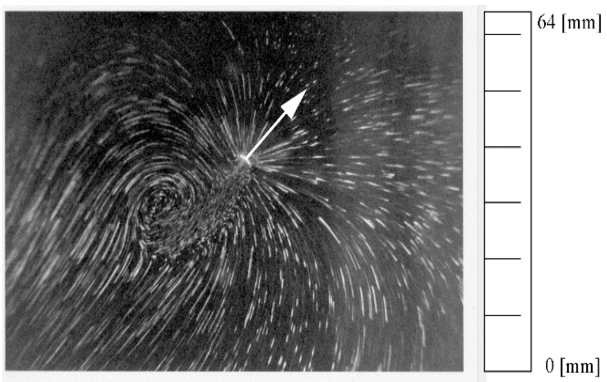

Fig. 7 flow field generated by 1.5 mm diameter bubble trains in X-Y plane

The whole flow field is attracted from right and left regions, towards the triangle and vortex region. The vortex region is considered to be generated by the instabilities due to the two counter flows. The flow in the triangle region, which is generated in the opposite direction from the bubble motions, joins the flow attracted in the direction to the triangle region in the vicinity of the edge of the triangle region.

IV. Conclusion

The effects of mutual distance of bubbles, the bubble diameter and the bubble rising velocity of the bubbles on the behaviors of the both bubble trains itself and the flow field were investigated with the single nozzle by changing only the nozzle upstream pressure.

The mutual distances and generation frequency of the bubbles were found to be important parameters for the bubble coalescence, which leads to the transition of the structures of both the bubble trains and the flow field. The flow field development by the rising bubbles in the stagnant water was observed by the flow visualization procedure. It was found that the bubble trains with relatively simple structures are associated with the substantially complicated three-dimensional flow field around. By using this technique, the flow regions, which are generally as small as 10 mm/s could be measured successfully. This technique could be used in the region where normal flow measuring probes could not measure accurately, such as in the turbine/pump blades and casings.

References

[1] Katz, J. and Meneveau, C., 1996, Wake-induced relative motion of bubbles rising in line, *Int. J. Multiphase Flow*, Vol. 22, No. 2, p. 239.

[2] Yoshida, S. and Manasseh, R., 1997, Trajectories of Rising Bubbles, *Proc. 16th Multiphase Flow Symp*., p. 61.

[3] Murai, Y., Watanabe, S., Yamamoto, F. and Matsumoto, Y., 1997 Three-dimensional measurement of bubble motions in bubble plume using stereo image processing, *Int. Workshop on PIV'97-Fukui*, p. 13.

[4] White, F. M., 1986, *Fluid Mechanics*, McGraw-Hill Book Company.

[5] Haberman, W. L. and Morton, R. K., 1956, An experimental study of bubbles moving in Liquids, *Trans. ASCE*, Vol. 121, p. 227.

[6] Hartunian, R. A. and Sears, W. R. 1957, On the instability of small gas bubbles moving uniformly in viscous liquids, *J. Fluid Mech*. Vol. 3, p. 27

[7] Liu, W., Clark Nigel n. and Karamavruç A. I., 1997, Relationship between bubble size distributions and chord-length distribution in heterogeneously bubbling system, *Chemical Engineering Science* p.1267

[8] Churchill, S. W., 1988, *Viscous Flows*, Series in Chemical Engineering, Butterworths

[9] Saffman, P.G., 1956, on the rise of small air bubbles in water, *J. Fluid Mech*. Vol. 1, p. 249

[10] Peebles, F.N. and Garber, H.J., 1953, Studies on the motion of gas bubbles in liquids, *Chemical Engineering Progress*, Vol. 49-2, p 88.

Author's Profile

Rajendra Shrestha is Associate Professor of Fluid and Energy in Department of Mechanical Engineering, Pulchowk Campus, Institute of Engineering, Tribhuvan university, Nepal. Completed doctorate of engineering from Kyushu University, Japan in 2000. Supervising three PhD students and supervised more than forty five bachelor and master projects and thesis. More than thirty research papers in Journals and conferences.